PARTICULATE COMPOSITE ON THE BASIS OF HA AND TCP MICROPARTICLES AND NANOPARTICLES AS A POSSIBLE BIOMATERIAL FOR SPINE THERAPY

ŠÁRKA RÝGLOVÁ*#, ZBYNĚK SUCHARDA*, MARTIN ČERNÝ*, TOMÁŠ SUCHÝ*,**, MONIKA ŠUPOVÁ*, MARGIT ŽALOUDKOVÁ*

*Institute of Rock Structure and Mechanics v.v.i., ASCR, Department of Composite and Carbon Materials, V Holešovičkách 41, 182 09 Prague, Czech Republic
** Laboratory of Biomechanics, Czech Technical University, Faculty of Mechanical Engineering, Department of Mechanics, Biomechanics and Mechatronics, Technická 4, 166 07 Prague, Czech Republic

#Corresponding author, e-mail: ryglova@irsm.cas.cz

Submitted August 27, 2010; accepted November 12, 2010

Keywords: Particulate composite, Preparation, Hydroxyapatite, Tricalcium phosphate, Polydimethylsiloxane, Compressive strength

The aim of this experimental work was to propose a technology for preparing a particle-reinforced composite based on thermosetting polydimethylsiloxane resin matrix (PDMS) reinforced with hydroxyapatite (HA) or tricalciumphosphate (TCP) microparticles/nanoparticles for application as an intervertebral filling biomaterial situated inside a load-bearing PEEK cage. In addition, we determined the effect of microparticle and nanoparticle additives (HA, TCP) on the mechanical characteristics of the particulate composite, namely modulus of elasticity in compression (E_c) and compressive strength (σ). In this work, the proposed technology for preparing these particle composites with a thermosetting matrix functioned quite satisfactorily. We can conclude that with rising volume of the particle composite filling up to 25 vol.%, the E_c and σ_{cM} also rose to twice the values for the pure PDMS matrix. The effect of nanoparticles on the mechanical properties was more pronounced.

INTRODUCTION

Degenerative diseases are among the most widely spread diseases of civilization. One of main methods used in spinal therapy involves replacing a damaged disc by a graft and then fusing the two adjacent vertebrae. When it is not possible or not suitable to use a bone graft of organic source, the treatment is to use synthetic implants made of various certified materials, either monolite or composite. The most widely used materials are made of ceramics (bioglass) or corundum, alloys based on Co, Cr, Mo, Ni, W, Ti and its alloys, and thermoplastic polymers. Biomaterials containing HA, TCP, chitosane, PLLA, PVA, collagene, etc., are other materials that are reported to be in the research or clinical testing stage, and the results are promising [1,2,3-8]. The mechanical properties of an HA/polymer composite correspond to the mechanical strength of cortical bone better than "biomonolite" materials [9], and so the risk of stress-shielding is minimized.

Metal (often Ti) cages are widely used in present-day spine therapy. However, efforts are being made to use a non-metallic material in order to avoid excessive stiffness, potential allergic responses, and implant migration. For example, recently reported non-metallic materials made of bioabsorbable PLLA [2] or HA/collagen composite combined with rhBMP proteine [3] or PEEK used in our study[10].

Generally, on the basis of recent research reports, nanocomposites seem to be promising materials for further research and development of synthetic bone grafts.

Preparation of a particle composite on the basis of CaP particles (and polysiloxane)

During preparation, it is necessary to solve the common problem of particle agglomeration, which is caused by van der Waals interactions among particle molecules that lead to the creation of a non-homogeneous composite, leading to non-ideal particle dispersion [11].

The most usual way to prepare particulate composites is by using a common technology such as moulding and pressing a powder mixture of components [12], admixing bioceramic particles to a polymer matrix

with subsequent common plastic technology processing [13], using a colloidal way (mixing suspensions containing a polymer dispersant with subsequent dehydratation of the mixture) [11]. There are also reports of novel nanocomposite preparation technologies, e.g. freezing, gas-foaming (leading to the formation of a sponge-like porous composite) [14], thermally-induced phase separation (a solvent with a low melting point must be used, and this solvent is subsequently sublimated and a porous scaffold is formed) [14], preparation of a so-called interpenetrating composite (preparation of a porous ceramic scaffold with sequent impregnation of the polymer, perhaps with another ingredient to improve the compressive strength) [15], in-situ formation (nanoparticles are generated from precursors built in a polymer matrix, e.g. HA/polyamide 66, which is reported to achieve mechanical properties comparable to those of bone) [16,17], ex-situ formation (nanoparticles with a polymer shell incorporated into a polymer matrix) [18], preparation of a nanofibre composite [14].

Another way to prevent undesirable particle agglomeration is to apply various surface modifications of ceramic particles to improve the interface properties. Hovewer, many of these applications lead to use higher amounts of harmful organic solvents [13]. Pure mechanical mixing and ultrasonic energy provide only a temporary effect. There is particle settlement and agglomeration occurs again.

In order to achieve more permanent colloidal stability, many modifications have been made, mainly resulting in greater stability. For example, adsorption of Ca^{2+}, PO_4^{3-}, citrate ions improves the colloidal stability of HA. A chemical way to modify the HA surface can be provided, e.g., by re-esterification of the HA surface acid functional group with dodecylalcohol [19], incorporation of silanole groups (Si-OH) on the HA surface, or by silica (SiO_2) enabling the creation of a strong bond between HA and the polymer matrix [20], by PCL [21], by oleic acid [22], etc. It seems to be important to follow the proper preparation sequence. For example, simply adding oleic acid into a composite mixture does not improve the desired properties so much as adding the oleic acid separately into the solvent with HA, and then mixing with the polymer [22].

Several attempts to achieve good dispersion of ceramic particles have been successful, but the mechanical properties of most of these composites, mainly the compressive strength, have not been sufficient for load applications. In addition, some of them have revealed potential toxicity owing to their degradation products.

Due to various composite preparation difficulties, alternative ways have been investigated to prepare a biocomposite by tissue engineering or by seeking a biomimetic way, aimed at mimicking the excellent properties of natural organization. For example, an HA/collagen composite was prepared in this way [23,24].

EXPERIMENTAL

Hydroxyapatite (HA) and composites

Owing to the mechanical properties of HA, materials based on it are promising for use as regenerative implants for stimulating or accelerating bone healing, or for applications in low-load parts, e.g. the orbital floor, or as a bone defect filling material, a metal implant coating, or as supporters for drugs and molecules [10]. Stoichometric HA has low resorbability, which is a limiting factor for bone formation [25], and many experiments have been carried out in an attempt improve its resorption, e.g. substitution of OH^- (type A) or PO_4^{3-} (type B) in HA by CO_3^{2-} ions [26]. Substitution by silica also led to an improvement in this field [27]. Natural HA is not exactly stoichiometric, since its phosphate or hydroxy groups are replaced by other ions. In recent years, several composites based on HA have been reported [e.g., 28], for example composites with a bio-active glass, polymer or other ceramic matrix. HA coating of metal implants is also often used, mainly on Ti-alloys metals. So far, however, it seems that higher mechanical strength (and reliability) is accompanied by lower biocompatibility.

Tricalciumphosphate (TCP) and composites

In contrast to HA, TCP is unstable and highly soluble. It transforms to more stable HA after some time. It is more degradable than HA, and it disappears from the implant site as the new bone gradually grows. The degradation mechanism of TCP is based on chemical dissolution, unlike HA crystals, which dissolve after the release of protons from cell acidification [29]. The use of TCP ceramics tends to be focused on rapid resorbing applications [29]. In [30], there is a sugestion that the problem of the high dissolubility of β-TCP can be solved by magnesium modification, leading to the formation of β-TCMP, which is more resistant to hydrolysis and does not transform to HA so easily. Examples of bioresorbable composites are TCP/collagen, TCP/PLA, TCP/PCL composite, etc.

Polydimethylsiloxane (PDMS)

Reports of recent investigations have shown that glass fiber reinforced composites with a polysiloxane precursor matrix are promising candidates for bone replacement applications. In addition, they are not expensive [31]. PDMS has often been used in various medical applications for more than thirty years. Its indispensable advantage is its neutral light colour, so that it can be used for subcutaneous implants, in orthopedics, in maxillofacial reconstructions, or in finger-joint implants [32].

Reports have also shown that PDMS is a practically bioinert, non-toxic material. The presence of some particles in PDMS influences its biocompatibility and haemocompatibility. PDMS can be directly produced in medical quality, and there is no need to add other components for curing [32,33].

In this experimental work, we used the trademarked Lukosil M130 polysiloxane resin, supplied by LUČEBNÍ ZÁVODY KOLÍN (Czech Republic). Lukosil M130 is a 50 % solution of polydimethylsiloxane in xylene. It provides good stability even over long-term storage, and the polymer is sufficiently homogeneous for composites made of it to perform final mechanical properties in a satisfactory range[34].

Micro/nanohydroxyapatite (50-150 μm, 100 nm and 20-70 nm) and micro/nano tricalcium phosphate (50-150 μm and 100 nm) particles, supplied by Berkeley Advanced Biomaterials, Inc. (Berkeley, CA, USA), were applied as a material for particle reinforcement. These particles are commonly produced by this company for use in medical applications.

Technology for preparing a particle composite with a thermosetting matrix was set up after a series of experiments. The technological steps were as follows.

In order to achieve good penetration, the particles are first mixed in a resin solution for at least 8 hrs, with subsequent solvent evaporation at 60°C in a vacuum for a minimum of 12 hrs. Then the intermediate product is homogenized in a kneader at room temperature for 18-24 hrs.

The mould is put into a pressing form and is initially heated at 130°C for 2 hrs. On the basis of previous tests, we set up a curing programme, raising the temperature step by step from 160-250°C and raising the pressure step by step to 0,5 MPa, with an overall curing time of up to 24 hrs.

Experimental methods

Some of the samples were investigated by ima-ge analysis, using a NIKON Optiphot-100S light microscope with a JENOPTIK (Germany) digital colour camera with the NIS-ELEMENT AR 2.30 imaging system (Laboratory Imaging Prague) - mainly samples with microparticles), and also using a QUANTA 450 electron SEM microscope (FEI Company, USA), under a high vacuum, with an Au coating film on the samples.

In the image analysis, we monitored particle dispergation, the presence, character and size of the aggregates, pores or fissures/cracks. The influence of these monitored parameters both on particle dispergation in the matrix and on final composite mechanical properties was also examined.

The crystallite size *Lc* was calculated using the (002) basal diffraction peak ~ 30° 2Θ, hence the clear profile and independence of the line is favorable. The crystallite size and the distribution of crystallite size were calculated using MUDMASTER SOFTWARE [35], applying the Warren-Averbach [36] approach.

The chemical structure and the presence of functional groups was determined by Protégé 460 E.S.P. Infrared Spectroscopy, at an extension of 4000-400cm^{-1}, resolution 2 cm^{-1} and on an average 32 scans for KBR pellets and 64 scans for ATR mode, respectively.

The compressive elastic module E_c and the compressive strength σ were measured. The measurements were provided by an Inspekt instrument with a 50 kN load cell (Hegewald-Peschke, BRD). Sample deformation was monitored by two FMA extensometers. Al these measurements were provided in accordance with ČSN EN ISO 604, which is also acceptable for filled and reinforced reactoplasts (resinoids). The samples for testing were in cylindrical form, about 10 mm in height and 13 mm in diameter.

The statistical analysis was performed on the basis of non-parametric tests *(Kruskal-Wallis, Mann-Whitney*), finally finding a simple regression line to formulate the effect of particle filling on the mechanical properties of the composite.

Sample preparation

Polysiloxane resin is a thermosetting polymer, i.e. with rising temperature it begins networking (curing). This is an irreversible process. Due to this fact, it differs greatly from thermoplastic polymers, which can be processed repeatedly. So the possibilities of processing thermosetting and thermoplastic polymers are very different. Most of the reports in the introduction to this paper deal with the preparation of biocomposites with a thermoplastic matrix. Only a few reports deal with particulate composites with polydimethylsiloxane or, generally, with a thermosetting matrix for medical purposes.

First of all, it is necessary to reduce the primary volatile components in the moulding compound as much as possible. Then, during polycondensation the optimal curing programme needs to be set up to ensure that the gradually rising and released by-products of the networking reaction do not destroy the mould compact that is just originating. Here, several negative tendencies occur which counteract homogeneous particle dispersion. There is dense, particle hydrophilicity together with matrix hydrophobicity, influencing the mutual affinity and finally the coherent effect of temporarily lowered resin viscosity at elevated temperatures up to 160-200°C. All these factors lead to undesirable effects, namely particle settlement in a stationary state (e.g. during stationary pressing) or the formation of microaggregates of polar particles in a non-polar matrix.

It is not sufficient only to admix the particles into the resin, as particle settlement occurs within a relatively short time. In the following step, it is neccessary to

remove the solvent to prevent the formation of high porosity and cracks in the moulding compound due to solvent vaporization during curing. To achieve good dispersion of the particle filling after the solvent has been removed, the intermediate product has to be kneaded at room temperature. In brief, the nanoparticles are more stable and do not settle, while the microparticles tend to settle, particularly at lower filling concentrations.

On the basis of a large number of simple but time-consuming experiments, we were able to show that the appropriate thermal mode for curing the block moulding compound is from 160°C, slowly and gradually rising to 210-220°C at a cumulative exposition time of up to 24 hrs.

The exposition time can be shortened by organizing the curing mode with gradually rising temperature and gradually rising pressure, which reduces the volume of the aqueous vapour that is forming, but it sometimes remains enclosed inside the bulk and forms internal pores. Its whole volume fraction does not exceed 5-10 vol.% of the bulk volume. The technology requires the application of accurate and enclosed compression mould forms. The particles have a favourable effect, and are capable of adsorbing some of the aqueous vapor that forms. It seems to be advantageous to apply the greatest possible pressure, but the viscosity of the resin decreases as the temperature rises, and each component of the bulk has different thermal expansivity. There is therefore a risk of loss of the moulding mixture due to moulding form micro-untightness.

RESULTS AND DISCUSSION

Optical microscopy

The layer of settled particles occurred mainly in a microparticulate composite with filling volume fraction up to 15-20 %. At a higher filling volume, this phenomenon disappeared, but a higher occurrence of large pores was observed (Figures 1a,b). In the case of a nanoparticulate composite, particle settlement did not occur in almost the whole filling volume range, and only composites with higher filling tended to aggregate the particles (the smaller the particle, the bigger the aggregates) and to form small pores, but the homogeneity of the composite bulk was still preserved (see Figure 1c).

As more particles are added, the viscosity of the moulding compound rises. When this mould is heated, its viscosity first decreases and then after the start-up of polycondensation the mould viscosity begins to rise again. In the case of a lower particle volume fraction, the viscosity of this mould is too low, so the particles have enough time to settle before the matrix network forms. By contrast, when there is a higher volume fraction and smaller particles, the higher viscosity of the mould retards particle movement in the direction of the gravity. In the case of nanocomposites with a lower particle volume fraction, the stability of the particles may be due to the generally larger interface area, so the whole surface friction drag rises, and no influence of the temporarily lowered matrix (mould) viscosity can appear in practice.

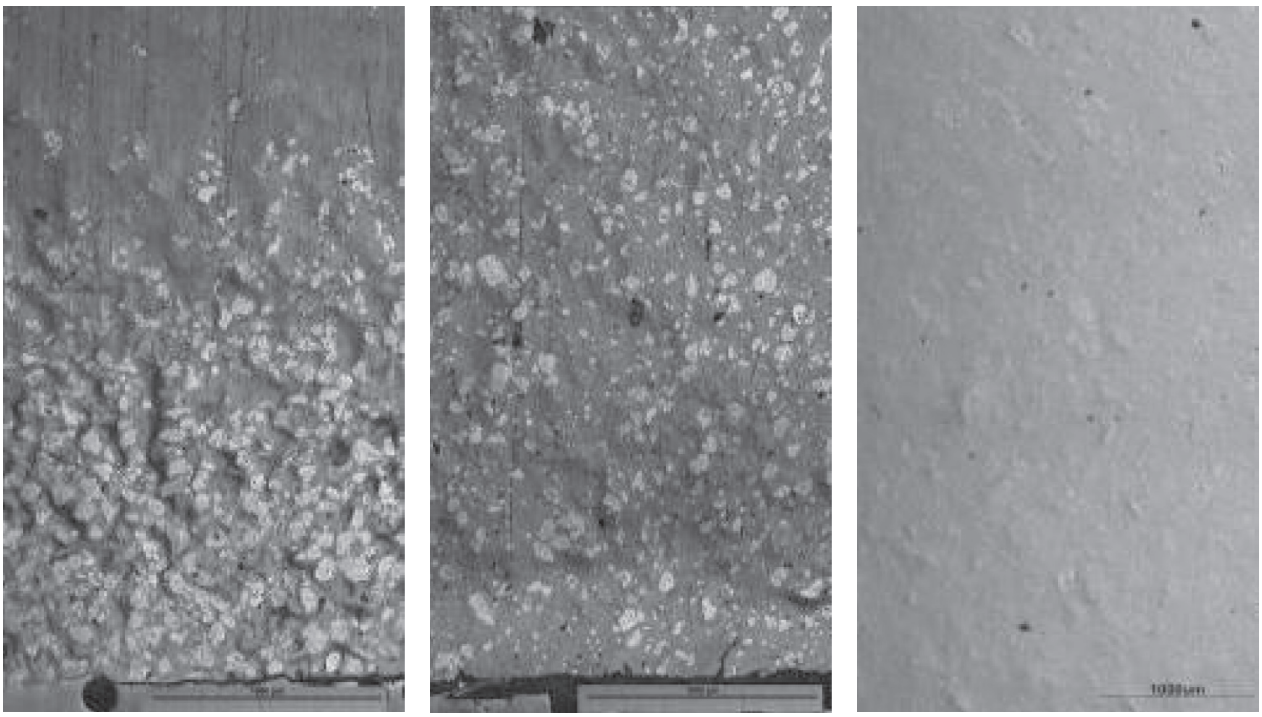

a) M5 (particle filling 5 vol.%) b) M20 (particle filling 20 vol.%) c) NN20 (particle filling 20 vol.%)

Figure 1. Optical micrographs of the longtudinal cut of the sample.

The figures below show examples of the most frequent damage type of samples after undergoing compressive tests. Longitudinal cracks occurred mostly in low particle content samples (Figure 2a), and backsliding occurred in samples with a higher particle volume content (Figure 2b). In addition, the microparticulate samples had a greater tendency than the nanoparticulate samples to slide back partially. Series of samples with lower compressive values (NN, MF) largely slid back throughout the range of the filling volume.

a) N5, slight longitudinal crack

b) N25, the sample is sliding back

Figure 2. Optical micrographs of the samples after compression tests.

Scanning electron microscopy

SEM analysis showed an evident contrast among the samples with a range of filling volume ratios and particle types. In the case of nanoparticle samples a different structure of the "inner surface" was ob-served, both for composites with hydroxyapatite par-ticles (samples N and NN) and for composites with tricalciumphosphate particles (samples NF). Samples with HA (Figures 3 a,b) show a rather "indiscrete relief". HA crystallities and PDMS matrix protrusions are similar in size. HA particles appear to be round in shape, partially covered or embedded into the matrix, with no evidence of a sharp interface boundary. Unlike samples with HA, samples with TCP particles (Figures 3 e,f) show a markedly structured inner surface, with very articulated particles that are roughly uniformly spread. NN samples with HA 20-70 nm, (Figures 3 c,d) somewhat resemble N samples (with HA 50-150 nm), but their inner surface appears to be even "less structured" than that of samples N.

In the case of microparticles (Figure 4), the recapitulation is not so definite. No very pronounced differences in appearance among composite samples with various particle types were observed, especially in the case of low-filled samples. The higher the particle filling, the more pronounced the difference in appearance. But the question arises: Was this influenced by the use of the specific particle type in the matrix, or by the particle size and the particle filling volume ratio? It seems that the application of a greater particle size together with a higher filling volume leads to more samples with defects (presence of aggregates, high level of stress in a brittle matrix in aggregated areas, critical crack length is easily reached and cracks propagate easily.

The results of the mechanical tests on the samples also proved that there is a significant difference in compressive strength, e.g. for samples M20 and M25 (HA particles), which also show a disimilar SEM appearance (see Figures 4 b,c), where M20 still appears to be plastic, with more or less widespread particles, without any marks of major failures. Unlike the case of M20, for sample M25 aggregates, cracks and backslidden parts of the matrix/particles were observed.

Samples with tricalciumphosphate particles showed a similar tendency in appearance as in the "HA" samples, but the tendency was less pronounced.

We can summarize that the 5 % particle filling samples generally showed a more plastic and less articulated inner surface in contrast to the 25 % (or 20 %) particle filling samples. Higher particle filling may evoke a more structured and therefore a more crystallic inner appearance. It can be stated that the higher the particle filling the more structured the surface, while the relative matrix fraction decreases. It is apparent that the use of particles of large size (microsize degree) together with high particle filling leads to the creation of samples with less resistance to the formation of technological faults, and therefore with less mechanical strength, e.g., in compression.

The use of a different particle type also led to a marked contrast in SEM appearance, mainly of the nanoparticle samples. The higher the particle filling, the more pronouced the difference between the particle types.

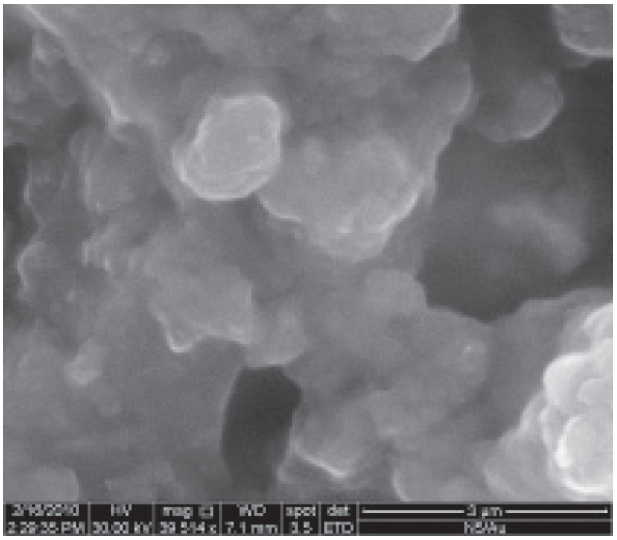

a) N5 (5 vol.% of HA, 100 nm)

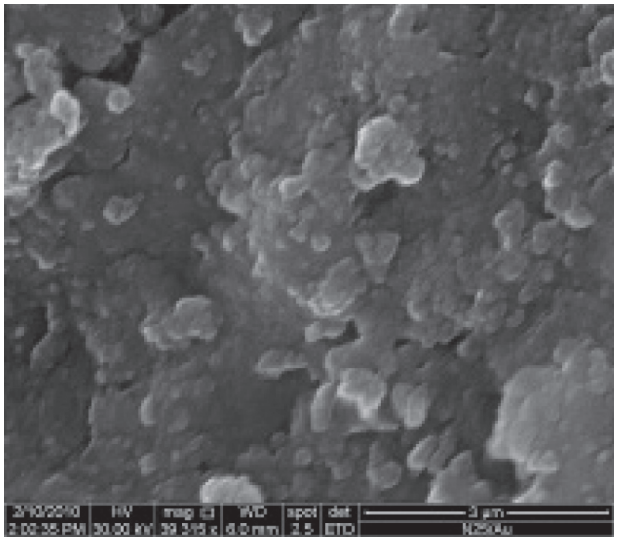

b) N25 (25 vol.% of HA, 100 nm)

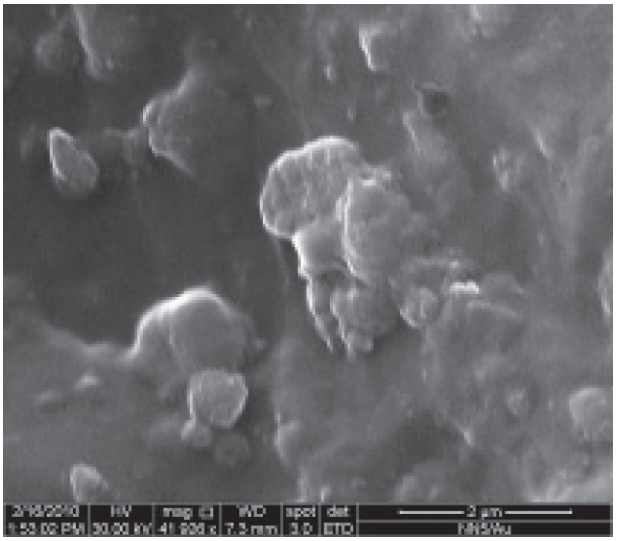

c) NN5 (5 vol.% of HA 20-70 nm)

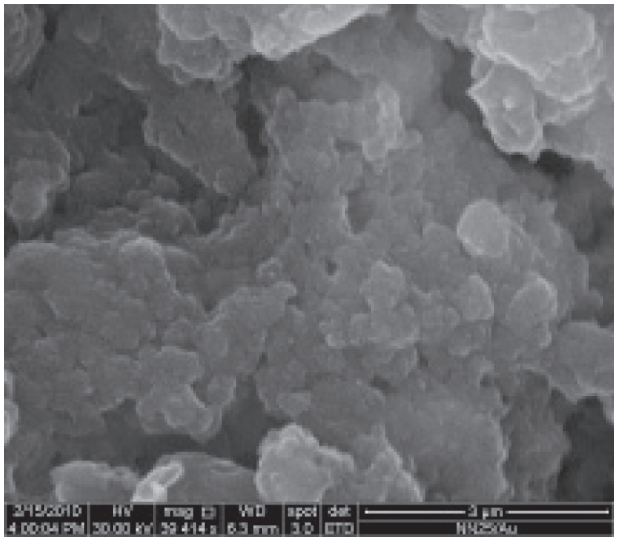

d) NN25 (25 vol.% of HA 20-70 nm)

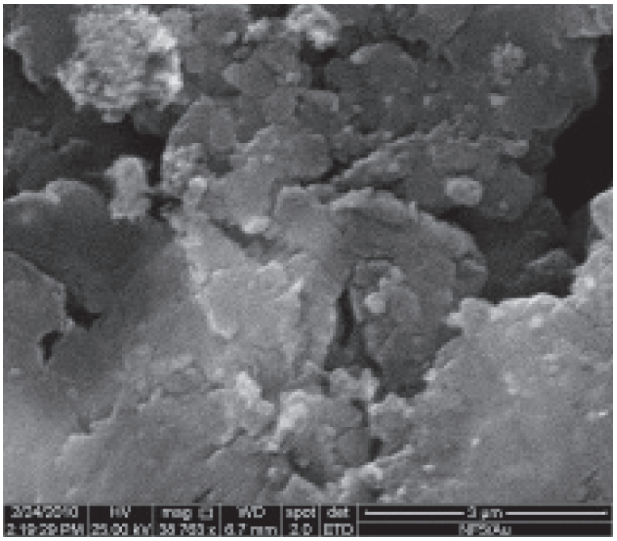

e) NF5 (5 vol.% of TCP, 100 nm)

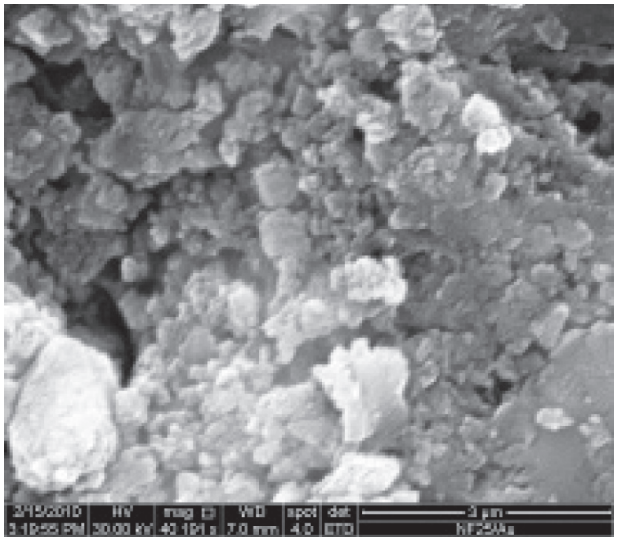

f) NF25 (25 vol.% of TCP, 100 nm)

Figure 3. SEM micrographs of a composite with a polydimethylsiloxane matrix and HA or TCP nanoparticles (N, NN - with nano HA particles, NF - with nano TCP particles).

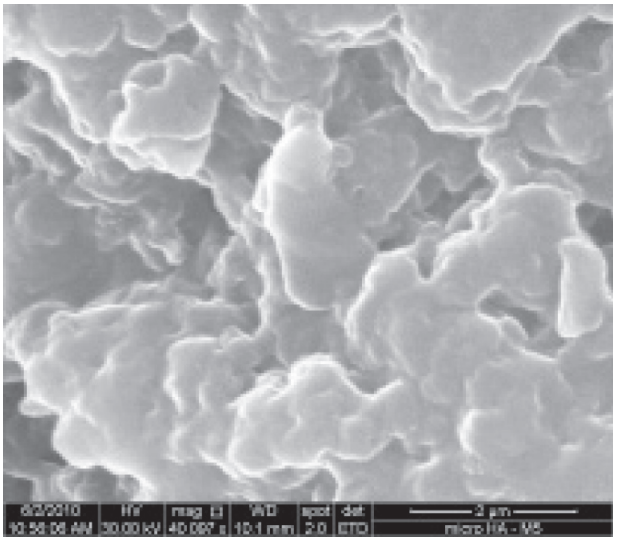

a) M5 (5 vol.% of HA, 50-150 μm)

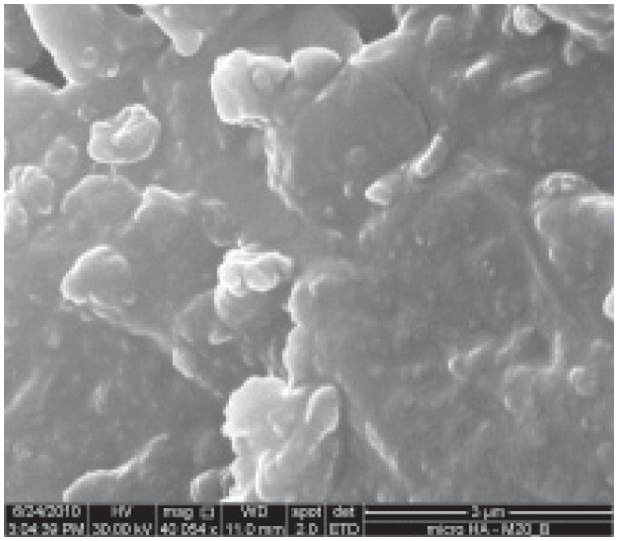

b) M20 (20 vol.% of HA 50-150 μm)

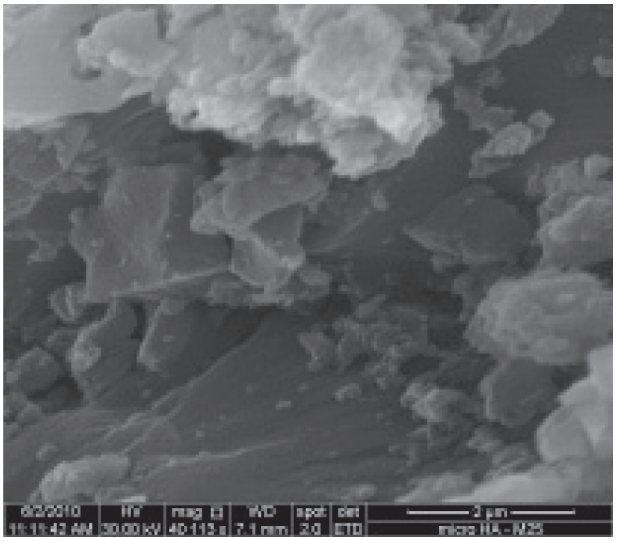

c) M25 (25 vol.% of HA, 50-150 μm)

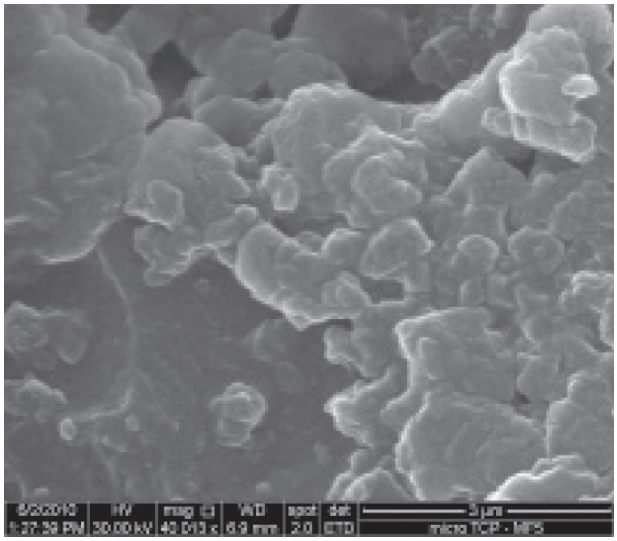

d) MF5 (5 vol.% of HA, 50-150 μm)

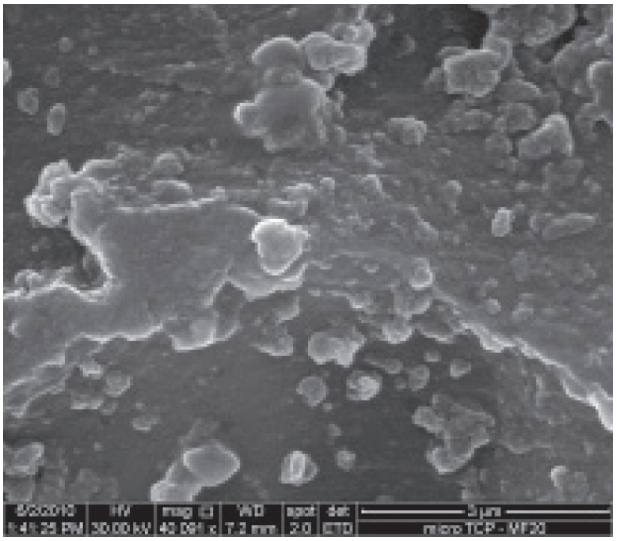

e) MF20 (20 vol.% of TCP, 50-150 μm)

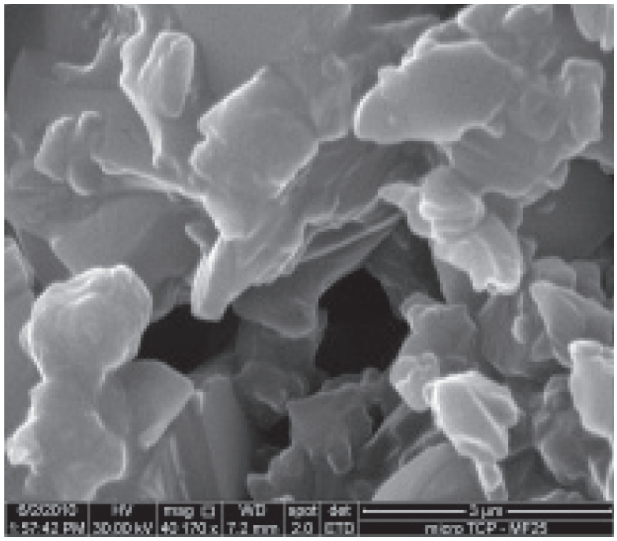

f) MF25 (25 vol.% of TCP, 50-150 μm)

Figure 4. SEM micrographs of a composite with a polydimethylsiloxane matrix and HA or TCP microparticles (M - with micro HA particles, MF - with micro TCP particles).

Analysis of particle size

Crystallite size is defined as the size of a well-ordered molecular domain that diffracts in phase. Using the Warren-Averbach method (average of the column length), the results differed from the crystallite sizes evaluated from the Scherrer equation (volumetric average of crystallite size), which is used for specimens in which lattice strain is assumed to be absent (domain size = particle size). The area-weighted frequency means crystallite size <Lc> calculated from the distribution and crystallite size distributions for all types of hydroxyapatite and calcium phosphate particles are given in Table 1.

Table 1 shows that the average crystallite size of the nHA sample (N) is significantly lower than the others (M, MF, NF). The crystallite size distribution curve (sample N) has two major maxima, and most of the crystallites are in the range from 8 to 26 nm. Larger domains are represented with sizes around 33 nm, and the crystallites are rather small and uniform. Below 8 nm the amount of crystallites is negligible for sample N.

For the other samples M, MF, NF these values represent the negligible amounts of crystallites 20, 15 and 17, respectively. The distribution curves of these samples have higher frequencies of larger domains. The calculated log-normal distribution (solid line) roughly traces the character of the distribution of the filler samples. For comparison, the average crystallite size Lc of human bone, studied by Handschin and Stern [37], has been determined as 28 nm within the age group 0-25, reaching a constant average domain size of 34 nm within age group 30-80. It has been reported that smaller crystallite size is connected with greater apatite solubility in bone [38].

Crystallinic analysis shows that nanoparticles display more pronounced differences than microparticles. We can assume that both variability in the technological preparation of each type of particle and the physio-chemical parameters of the HA or TCP particles influence the way that each molecule is arranged in the crystal domain space. Variations of domain arrangement may also influence the boundary interface properties with the matrix, and therefore also the mechanical properties, and possibly the biological response.

Infrared spectroscopy

The spectra in the Figure 5 (C,D,E) show a very intensive and broad band at 950-1100 cm^{-1} (950-1250 cm^{-1} with KBr pellet), with the top peak of the band at 1040 cm^{-1}. This band corresponds to the stretching vibrations of the phosphate groups in HA. The double band at 555-610 cm^{-1} is associated with the deformation vibration of the phosphate groups, and the bands at 1950-2100 cm^{-1}(in the case of mHA only) are due to over-

Table 1. Crystallographic parameters of filler types.

Type of filler	Average of crystallite size (nm)	Position 2Θ (°)	Crystallite size distribution
M	50.4	30.159	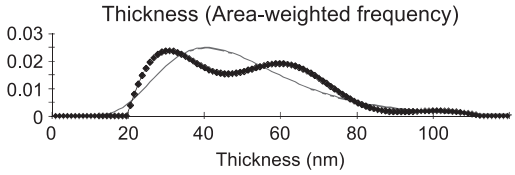
N	28.8	30.192	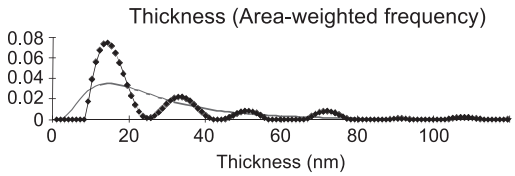
MF	48.7	30.077	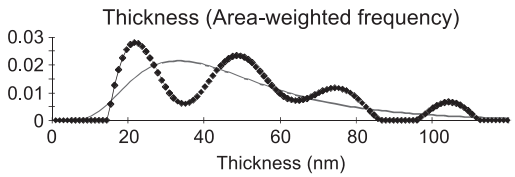
NF	53.4	30.079	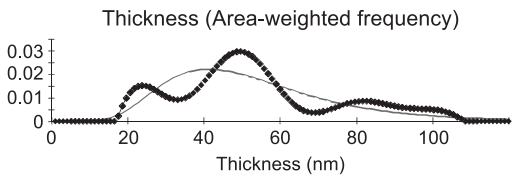

toned/combined vibrations of phosphate [19]. In contrast to the spectrum of mHA, the spectra of nHA, nnHA where bands around 1454,1421 and 875 cm^{-1} occurred, indicate the presence of carbonate groups in these HA, indicating substitution of carbonate ions into the HA. The carbonate peaks at 1454-1421 cm^{-1} are assigned to the A- and B- substitution types, and the peak at 875 cm^{-1} is associated with the labile surface carbonate. The carbonate content was calculated from the ratio of certain carbonate and phosphate peaks in the way reported in [39]. The calculated carbonate content in the nHA and in the nnHA was 1.5-2 % and 2.6-2.75 %, respectively.

It has been reported that a small amount of carbonate ions substituted into the HA lattice improves the mechanical strength [39]. Not only the HA crystal surface structure but also its solubility and bulk growth morphology favouring platelets other than needles is influenced by CO_3^{2-} substitution into HA. The collagen fibrils interact better with the HA platelet form than with the needle form [40].

Similarly as in the case of HA, the spectrum of TCP in the Figure 18 (A,B) showed a very intensive and broad band at 900-1120 cm^{-1} (850-1400 cm^{-1} with KBr pellets), with the top peak of the band at 1045 cm^{-1}, indicating the stretching vibrations of the phosphate groups in TCP. The double band at 550-610 cm^{-1} is associated with the deformation vibration of the phosphate groups, and the bands at 1900-2150 cm^{-1} (in the case of mTCP only) are due to overtoned/combined vibrations of phosphate. In contrast to nTCP, the peak at 724 cm^{-1} occurring in the spectrum of mTCP may indicate the presence of traces of $P_2O_7^{4-}$ (pyrophosphate) [41].

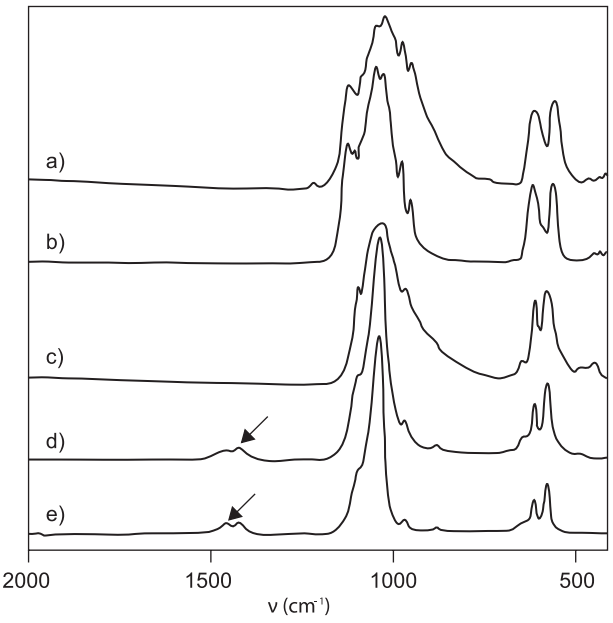

Figure 5. Infrared spectra of hydroxyapatite and tricalcium phosphate (below 2000 cm^{-1}, measured in the ATR mode); a) mTCP, b) nTCP, c) mHA, d) nHA, e) nnHA. Arrow keys point to the presence of carbonate groups in nHA and nnHA.

The IR spectra that were obtained proved the presence of carbonate ions in the case of HA nanoparticles and the presence of pyrophosphate ions in the case of TCP microparticles. These may have been caused by the technical production by-product residues of each particle group. Each single ingredient of the particle (mainly nHA and nnHA) influences either its chemical composition or its surface topology, thus modifying the crystal growing morphology, which can then influence the way in which the interactions at the interface between particle and matrix take place, resulting in the final mechanical properties of the composite.

It should be noted that the spectra of HA or TCP microparticles displayed a very broad band around 1040 cm^{-1} with overtoned/combined bands of phosphate ion, but the spectra of the nanoparticles did not show such a broad band as that shown by the micro band. The spectra observed in the ATR crystal mode displayed the same effect, but with less intensity. This band broadening effect is probably caused by the particle sample size, which may influence the amount of light dispersion.

Mechanical properties

Compressive tests were applied to evaluate the mechanical properties. Compressive tests were chosen due to the assumed application of these particle composites mainly under compressive stress. The measured and averaged values of modulus of elasticity in compression E_c and compressive strength σ, with its corresponding standard deviations, are displayed in Figures 6 and 7 respectively.

Elasticity module E_c

As assumed, E_c rises along the particle filling fraction over the series of sample type nHA, mHA, nTCP and mTCP. For most series of samples, the linear regression of the measured values with its confidence intervals suits well. This is confirmed by the fact that the micro and nanoparticles have a total reinforcing effect in the case of these composite types, reaching values in the interval from 0.8-2.3 GPa, which is about one order of magnitude lower than the modulus value indicated for cortical bone.

However, if it is applied as an intervertebral cage filling, we can assume that the whole system will provide superior stiffness. It may be advantageous to be able to optimize the stiffness of the intervertebral spacer by filling it with one of the particle composites of lower stiffness that are under study. By modifying the stiffness of the intervertebral system we can avoid the disadvantage that an excessively rigid spacer does generate a stress-shielding effect, which lead to unphysiological bone remodeling process and can lead to loss of bone density, so that the intervertebral spacer can be broken through vertebrae bone.

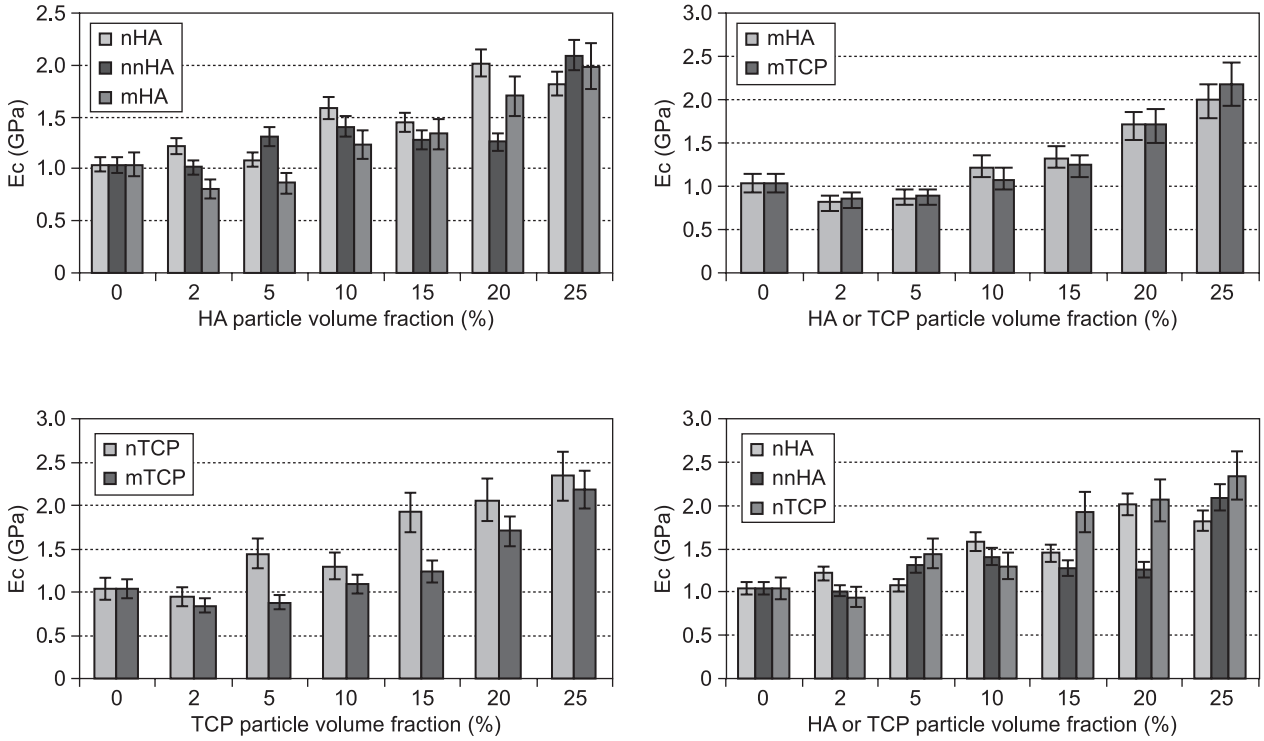

Figure 6. The elasticity module E_c of the composites vs. particle volume (nHA, nnHA - nano HA composite; mHA - micro HA composite; nTCP - nano TCP composite; mTCP - micro TCP composite).

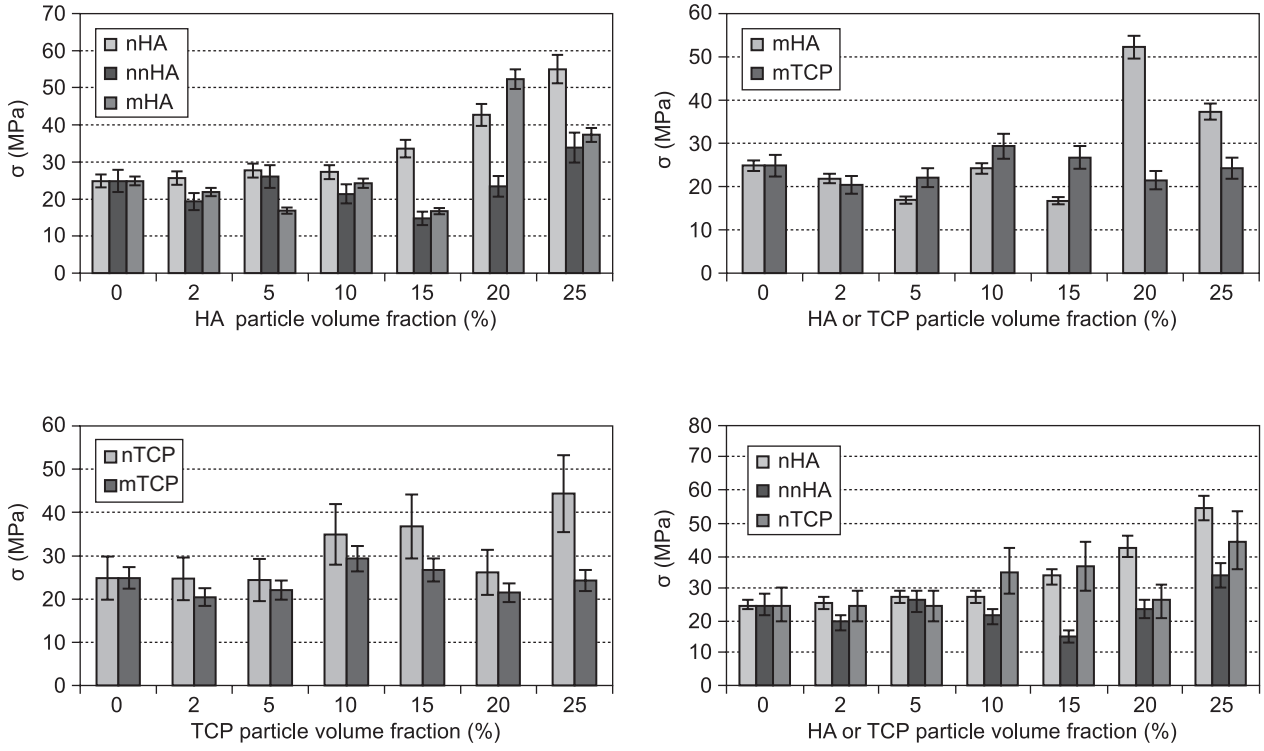

Figure 7. The compressive strength σ of the composites vs. particle volume (nHA, nnHA - nano HA composite; mHA - micro HA composite; nTCP - nano TCP composite; mTCP - micro TCP composite).

The effect of particle size and particle type on the E_c modulus values has not been proved statistically. We can summarize that the ratio of composite particle filling has a substantial effect on the compressive E_c modulus.

Compressive strength σ

We can summarize that nanocomposites nHA and nTCP mostly have greater compressive strength than microcomposites mHA and mTCP. This is in keeping with theoretical assumptions on interface interactions, i.e., the larger the surface, the larger the contact area, and therefore nanocomposites have a larger reinforcement-matrix interface than microcomposites. Thus, the greater number of interface interactions in nanocomposites than in microcomposites means that it takes a stronger impact to destroy the composite and that nanocomposites have greater compressive strength.

However, in most cases the particle strengthening effect rose until more than 10 % of the particle volume for nanoparticles, and there was a greater "shift" to 15-20 % for microparticles. This retardation of strengthening can be explained by the lower homogeneity of microcomposites (see the occurrence of particle settlement of the low particle filling ratio in the case of the composite in Figure 1a), where the rather destructive effect of non-homogeneity cannot be overcome by the particle reinforcement effect up to 15-20% volume filling.

In particular, nanoparticle samples reach compressive strength values up to 55 MPa, twice the levels of the values for the pure resin matrix. Generally, all series reached lower compressive strength values than the values for cortical bone, which is reported to reach up to 200 MPa. However, the values are higher than for spongious bone, which is reported to reach values of only units. In combination with a PEEK cage, which can achieve strength of 119 MPa [42], the intervertebral system should provide sufficient support for bone cell ingrowth the biocomposite filling.

The HA particulate composite (nHA, mHA) achieved a more satisfactory outcome than the TCP particulate composite, but the difference between the two sorts of composite was not very pronounced. This may be explained by the different character of the interface interactions between particle and matrix. Unlike TCP, hydroxyapatite (HA) in its basal crystallic form is composed of two molecules containing two OH groups, which enable bonding with another OH group of polysiloxane forming an -O- bond, hydrogen-bridging bond, respectively. Then the interface bonding quality is not so dependent on the extent of the interface surface as in the case of TCP, where only the effect of physical or electrostatic forces on the interface area may take place. This hypothesis of the effect of the chemical composition of the particles (particle type) leading to a different way of interacting with the matrix is supported by SEM photographs, which show differences in appearance. The tendency to change appearance was more pronounced for nanocomposites.

The series of nnHA-containing hydroxyapatite particles of 20-70 nm differs from the other series studied above. This dissimilarity can be explained by the apparently elevated hygroscopy of this particle type, which may be due to the relatively large particle interface surface, or due to bonding with a larger amount of water, which may be a polycondensation by-product of matrix curing and probably forms more pores and cracks of various sizes.

In addition, image analysis (see above) shows the tendency of NN particles to aggregate as more than one order of magnitude higher than in the case of the N particles. It should be appreciated that nnHA particles are at least two times smaller in grain size than nHA or nTCP, so the number of nnHA particles must be an order of magnitude higher than particles of N or NF per volume unit. In addition, nnHA particles are twice as wettable as nHA or nTCP particles.

It should be noted that a similar trend of compressive mechanical properties was reported for a fiber-reinforced composite with the same polysiloxane matrix and HA particle filling [43]. All these findings correspond to the used nanoparticles being hygroscopic and their equilibrium surface moisture being up to 2 wt.%. This may be due to the relative ratio of the surface/particle volume, which influences the surface physical and chemical proportions although the bulk chemical composition is the same. HA and TCP molecules are polar. Considering the polarity of the individual molecules, the nanoparticles still appear to have bulk polarity but the microparticles probably lose their bulk polarity as a consequence of the variously oriented crystal groups that have formed. It should be taken into account that the PDMS matrix is non-polar, and so the interface surface tension is rather high. The presence of water at the interface certainly decreases the interface bonding strength. In addition, the water released at an elevated temperature spreads into the interface forming microcracks and thus destroying the composite. This may explain why the differences between the microparticulate composite and the nanoparticulate composite are not so pronounced.

The analytical methods used here show that the invidual particle types differ from each other not only by their chemical composition and size, but also by their crystallinity, and by the amount of various ingredients probably imported by different technological production. The chemical composition and also the particle size and small amounts of ingredients can influence the particle surface topology, and also its crystallinity and its interface interaction with the matrix or live cells. These effects may suggest a way to produce the composite, and may affect the mechanical and biological response of the composite.

The statistical analysis showed that the particle filling volume ratio in the composite has a dominant effect on its final mechanical properties. Other parameters studied here, i.e. particle size, chemical composition, crystallinity and other additional parameters do not show such a strong effect on the short-term mechanical properties.

CONCLUSION

Reproducable technology for preparing a composite moulding compact with CaP particles and a polysiloxane matrix has been proposed. By taking into account the thermosetting property of the matrix and its curing programme in an effort to minimize defect formation, the probability of this material type being suitable for bone graft applications can be increased. Image analysis showed a higher particle filling volume, and when nanoparticles are used there is better particle homogenization in the composite. It has been proved that both nanoparticles and microparticles have a general reinforcing effect on the composites studied here. If applied as an intervertebral cage spacer filling, the system will probably show superior total stiffness. The compressive strength values σ of the composite were approximately twice as high as the pure matrix value. The nanocomposites achieved superior results. The observed compressive values range from the values indicated for spongious bone (several units up to 5 MPa) to the values for cortical bone (up to 200 MPa). The effect of CaP particle size and chemical type on compressive strength is not very pronounced. The novel idea of this biocomposite is the use of a siloxane matrix in a bulk particulate composite, where greater interaction can occur between the tissue and the bioactive particles in the composite. The main purpose of these particulate composite fillers is to serve as a built-up material for bone ingrowth through pores inside the material. After the disc is removed, the space is gradually filled, and then the two adjacent vertebrae are fused. The PEEK intervertebral cage should provide sufficient mechanical stability, especially in compression.

Acknowledgement

This study was supported by the Ministry of Industry and Trade of the Czech Republic Program – TANDEM, No. FT-TA3/131. Research on problems of spinal diseases focused on degenerative and post-traumatic states of the spine, applying findings in tissue engineering, vertebra biomechanics, osseointegration of artificial replacements and revising their failures, was supported by the Ministry of Education project Transdisciplinary Research in Biomedical Engineering II., No. MSM 6840770012.

References

1. Darwis D., Stasica P., Razzak M. T, Rosiak J. M.: Rad. Physics and Chemistry *63*, 539 (2002).
2. Vaccaro A.R., Singh K., Haid R., Kitchel S., Wuisman P., Taylor W., Branch C., Garfin S.: The Spine Journal *3*, 227 (2003).
3. Itoh S., Kikuchi M., Koyama Y., Takakuda K., Shinomiya K., Tanaka J.:Biomaterials *23*, 3919 (2002).
4. Green D., Walsh D., Mann S., Oreffo R.O.C.: Bone *30*, 810 (2002).
5. Marciniak J.: Engineering of Biomaterials *1*, 12 (1997).
6. Di Martino A., Sittinger M., Risbud M.V.: Biomaterials *26*, 5983 (2005).
7. Richardson S. M., Curran J. M., Chen R., Vaughan-Thomas A., Hunt J. A., Freemont A. J., Hoyland J. A.:Biomaterials *27*, 4069 (2006).
8. Green D., Walsh D., Mann S., Oreffo R.O.C.: Bone *30*, 810 (2002).
9. Murugan R., Ramakrishna S.: Comp. Sci. Tech. *65*, 2385 (2005).
10. Balík K., Suchý T., Sucharda Z., Rýglová Š., Denk F.: Ceramics-Silikaty *53*, 310 (2009).
11. Yasuda H.Y., Mahara S., Nishiyama T., Umakoshi Y.: Sci Technology Advanced Materials 3, 29 (2002).
12. Homaeigohar S.Sh., Yari Sadi A., Javadpour J., Khavandi A.: J. Eur. Ceram. Soc. *26*, 273 (2006).
13. Kang Y. et al.: Mater. Lett. *62*, 2029 (2008).
14. Šupová M.: J. Mater. Sci.: Mater. Med. *20*, 1201 (2009).
15. Miao X., Lim W.K., Juany X., Chen Y.: Mater. Lett. *59*, 4000 (2005).
16. Jie W., Yubao L.: Europ. Polymer J. *40*, 509 (2004).
17. Wang X., Li Y., Wei J., de Groot K.: Biomaterials *23*, 4787 (2002).
18. Rozenberg B.A., Tenne R.: Prog. Polym. Sci. *33*, 40 (2008).
19. Borum-Nicholas L., Wilson Jr. O.C.: Biomaterials *24*, 3671 (2003).
20. Borum-Nicholas L., Wilson Jr. O.C.: Biomaterials *24*, 3681 (2003).
21. Hong Jae L., Sung E. K., Hyung W. C., Chan W. K., Kyung Ja K., Sang Cheon L.: Europ. Polymer J. 43, 1602 (2007).
22. Kim H.W.: J. Biomed. Mater. Res. A *83*, 169 (2007).
23. Chang M.C., Tanaka J.: Biomaterials *23*, 3879 (2002).
24. Chang M.C., Tanaka J.: Biomaterials *23*, 4811 (2002).
25. Duchyenne P., Qiu Q.: Biomaterials *20*, 2287 (1999).
26. Murugan R., Ramakrishna S., Rao K.P.: Mater. Lett. *60*, 2844 (2006).
27. Damia C., Sharrock P.: Mater. Lett. *60*, 3192 (2006).
28. Suchánek W., Yoshimura M.: J. Mater. Res. *13*, 94 (1998).
29. Detsch R., Mayr H., Ziegler G.: Acta Biomater. *4*, 139 (2008).
30. Lee D., Sfeir C., Kumta P. N.: Materials Science and Engineering C *29*, 69 (2009).
31. Suchý T., Balík K., Černý M., Sochor M., Hulejová H., Pešáková V., Fenclová T. Ceramics-Silikaty *52*, 29 (2008).
32. Abbasi F., Mirzadeh H., Karban A.-A.: Polym. International *50*, 1279 (2001).
33. Hron P.: Polym int *52*, 1531(2003).
34. Rýglová Š., Sucharda Z., Balík K.: Ceramics-Silikaty *51*, 89 (2007).
35. Eberl DD, Drits V, Srodon J, Nüesch R.: U.S. Geological Survey Open File Report.; 96 (1996) revised 8/24/00.
36. Warren BE, Averbach BL.: J Appl Phys. *21*, 595 (1953).
37. Handschin RG, Stern WB.: Bone *16*, 355S (1995).
38. Tanaka H., Futaoka M., Hino R.: J Colloid Interface Sci *269*, 358 (2004).
39. Murugan R., Ramakrishna S., Panduranga Rao K.: Mater. Lett. *60*, 2844 (2006).
40. Wopenka B, Pasteris JD.: Mat Sci Eng C-Bio S *25*, 131 (2005).
41. Karlinsey R. L., Mackey A. C., Walker E. R., Frederick K. E..: Acta Biomater. *6*, 969 (2010).
42. Huttunen M., Ashammakhi N.., Törmälä P., Kellomäki M.: Acta Biomater. *2*, 575 (2006).
43. Suchý T., Balík K., Sucharda Z., Černý M., Sochor M.: Eng. Biomater. *1-2*, 69 (2007).